3-1985

Magnetic Field Effects in the Dynamics of Alternating and Anisotropic Quantum Spin Chains

James H. Taylor

Gerhard Müller
University of Rhode Island, gmuller@uri.edu

Citation/Publisher Attribution

James H. Taylor and Gerhard Müller. *Magnetic field effects in the dynamics of alternating and anisotropic quantum spin chains*. Physica 130A (1985), 1-33.
Available at: http://dx.doi.org/10.1016/0378-4371(85)90096-2

Magnetic field effects in the dynamics of alternating or anisotropic quantum spin chains

James H. Taylor[1] and Gerhard Müller[2]

[1] Department of Physics and Astronomy, The University of Toledo, Toledo, OH 43606, USA and Department of Physics, University of Rhode Island, Kingston RI 02881, USA

[2] Institute for Theoretical Physics, State University of New York at Stony Brook, Stony Brook, NY 11794, USA and Department of Physics, University of Rhode Island, Kingston RI 02881, USA

This is a study of magnetic-field effects on various zero-temperature properties of the one-dimensional $S = \frac{1}{2}$ XY model with exchange alternation or anisotropy. Alternation and anisotropy in the interaction cause different types of spin ordering in the ground state, which in turn are responsible for characteristic effects in various physical properties. The presence of an external magnetic field perpendicular to the xy-plane has the tendency to counteract these orderings. The latter are suppressed when the field reaches a critical strength. Various ground state properties of the two models are calculated, with emphasis on dynamic correlation functions. In some respects the alternating and the anisotropic models exhibit surprisingly similar properties, particularly in zero magnetic field. Important differences arise in other respects due to the different symmetry properties of the two models. Our calculations are exact and most results are presented as closed-form expressions.

1. Introduction

One-dimensional (1D) quantum spin models are known to exhibit interesting and nontrivial critical properties at zero temperature as functions of various parameters such as exchange or single-site anisotropy, exchange alternation or an external magnetic field [1-31]. In some cases, these models are amenable to a rigorous analysis; in most other cases, valuable results are derived from numerical calculations. Furthermore, there exist various mappings between such $T = 0$ critical behaviors and the critical behaviors of 2D classical models as a function of temperature [32-34]. Moreover, the most conspicuous features of the $T = 0$ critical properties of 1D quantum spin models have been observed to make their appearance in measurements of various low-temperature properties of quasi-1D magnetic compounds [35-48].

In this paper we shall concentrate on various $T = 0$ properties of the 1D $S = \frac{1}{2}$ spin models described by the following two Hamiltonians, with emphasis on dynamic correlation functions [49]:

$$\mathcal{H}_\gamma = J \sum_{l=1}^{N} \big[(1+\gamma) S_l^x S_{l+1}^x + (1-\gamma) S_l^y S_{l+1}^y + h S_l^z\big], \tag{1.1}$$

$$\mathcal{H}_\delta = J \sum_{l=1}^{N} \big[\{1-(-1)^l \delta\}\{S_l^x S_{l+1}^x + S_l^y S_{l+1}^y\} + h S_l^z\big]. \tag{1.2}$$

The Hamiltonian (1.1) describes an XY model with exchange anisotropy controlled by the parameter γ ($0 \le \gamma \le 1$). The case $\gamma = 1$ corresponds to the familiar transverse Ising model.

In the model described by Hamiltonian (1.2) the exchange interaction is always isotropic in the xy-plane but it is alternating in magnitude along the chain. The amount of alternation is controlled by the parameter δ ($0 \le \delta \le 1$). In the limit $\delta = 1$, this system reduces to an array of noninteracting dimers. That is why the effect of alternating exchange is frequently called dimerization. In both models, which are identical for $\gamma = \delta = 0$, we allow for the presence of a uniform magnetic field h in the z-direction. The relevance of 1D quantum spin Hamiltonians in the context of physical

realizations has been firmly established over the last two decades by the ever more successful efforts of coordination chemists and physicists to synthesize high-quality quasi-1D magnetic compounds. Today there exist a large number of physical realizations for a variety of 1D quantum spin models including models with exchange alternation and anisotropy [35-48].

Alternating spin chains, in particular, have gained prominence in the context of the study of quasi-1D magnetic compounds which undergo a spin-Peierls transition. The spin-Peierls transition is the magnetic analog of the familiar Peierls instability in electron-phonon systems: the exchange coupling between magnetic ions can induce under special circumstances a spontaneous distortion of the lattice such that nearest-neighbor magnetic ions move alternately closer and further apart [50].

Clearly, the model Hamiltonians (1.1) and (1.2) which we use for describing the properties of anisotropic and alternating quantum spin chains, respectively, are of a very special kind and, for most applications, would have to be modified; e.g. by the inclusion of an exchange term for the z-components of the spins. However, the results for models (1.1) and (1.2) can be considered to be representative, in terms of the degree of complexity in static and dynamic behavior expected, for 1D quantum spin chains in general.

The remainder of this paper is constituted as follows. In section 2 we describe the transformation from the spin system to a system of free fermions, obtaining such quantities as the single-fermion dispersion relations and the single- and double-fermion energy gaps for both chains. In section 3, we obtain explicit expressions for static properties of these systems, such as the ground state energies, magnetizations, and susceptibilities, and describe their behaviors. Particular attention is given to long-range order in the chains, especially the nonuniform order of the alternating chain. Included is a discussion of how the latter can arise in connection with lattice distortion. In section 4 we discuss the dynamic correlation functions for the chains, obtaining closed-form expressions for the alternating chain for all values of the applied field and in several cases of special interest for the anisotropic chain. A special relation among elliptic integrals of the third kind is derived in the appendix.

2. Fermion representation

It is well known that the Hamiltonians (1.1) and (1.2) can be mapped onto a system of noninteracting spinless fermions by means of three successive transformations [12,13,21,25]: the Jordan-Wigner transformation from local spin-$\frac{1}{2}$ operators S_l^x, S_l^y, S_l^z to local fermion creation and annihilation operators

$$S_l^+ = S_l^x + \mathrm{i}S_l^y = a_l^+ \exp\left[\mathrm{i}\pi \sum_{j<l} a_j^+ a_j\right], \tag{2.1a}$$

$$S_l^- = S_l^x - \mathrm{i}S_l^y = \exp\left[-\mathrm{i}\pi \sum_{j<l} a_j^+ a_j\right] a_l, \tag{2.1b}$$

$$S_l^z = a_l^+ a_l - \frac{1}{2}, \tag{2.1c}$$

followed by the Fourier transform to wave-number-dependent fermion operators

$$a_k^+ = N^{-1/2} \sum_{l=1}^{N} \mathrm{e}^{\mathrm{i}kl} a_l^+, \quad a_k = N^{-1/2} \sum_{l=1}^{N} \mathrm{e}^{-\mathrm{i}kl} a_l, \tag{2.2}$$

with $k = (2\pi/N)n$, $n = 0, 1, \ldots, N-1$, and a Bogoljubov transformation to be described below. The first two transformations lead to the bilinear fermion Hamiltonians ($J = 1$)

$$\mathcal{H}_\delta = \frac{1}{2}(a_k^+, a_{k+\pi}^+) \begin{pmatrix} h + \cos k & \mathrm{i}\delta \sin k \\ -\mathrm{i}\delta \sin k & h - \cos k \end{pmatrix} \begin{pmatrix} a_k \\ a_{k+\pi} \end{pmatrix} - \frac{1}{2}hN, \tag{2.3a}$$

$$\mathcal{H}_\gamma = \frac{1}{2}(a_k^+, a_{-k}) \begin{pmatrix} h+\cos k & \mathrm{i}\gamma \sin k \\ -\mathrm{i}\gamma \sin k & -h-\cos k \end{pmatrix} \begin{pmatrix} a_k \\ a_{-k}^+ \end{pmatrix}. \tag{2.3b}$$

These are brought into diagonal form:

$$\mathcal{H}_g = \frac{1}{2}\sum_k \omega_k^g \left[c_k^+ c_k - c_k c_k^+\right], \quad g = \delta, \gamma, \tag{2.4}$$

with

$$\omega_k^\delta = h + \mathrm{sgn}(\cos k)\sqrt{\cos^2 k + \delta^2 \sin^2 k}, \tag{2.5a}$$

$$\omega_k^\gamma = \mathrm{sgn}(h+\cos k)\sqrt{(h+\cos k)^2 + \gamma^2 \sin^2 k}, \tag{2.5b}$$

by applying to (2.3) the Bogoljubov transformation characterized by the unitary matrix

$$U_k^g = \begin{pmatrix} u_k^g & v_k^g \\ v_k^g & u_k^g \end{pmatrix}, \tag{2.6}$$

where

$$u_k^\delta = \frac{1}{\sqrt{2}}\sqrt{1 + \frac{\cos k}{\omega_k^\delta - h}}, \tag{2.7a}$$

$$u_k^\gamma = \frac{1}{\sqrt{2}}\sqrt{1 + \frac{h+\cos k}{\omega_k^\gamma}}, \tag{2.7b}$$

$$v_k^\delta = -\mathrm{i}\,\mathrm{sgn}(\sin 2k)\frac{1}{\sqrt{2}}\sqrt{1 - \frac{\cos k}{\omega_k^\delta - h}}, \tag{2.7c}$$

$$v_k^\gamma = -\mathrm{i}\,\mathrm{sgn}\left[\frac{\gamma \sin k}{h+\cos k}\right]\frac{1}{\sqrt{2}}\sqrt{1 - \frac{h+\cos k}{\omega_k^\gamma}}. \tag{2.7d}$$

In the diagonal Hamiltonian (2.4) the new fermion operators c_k^+, c_k, are given in terms of linear combinations of the old fermion operators a_k^+, a_k as follows:

$$c_k^+ = u_k^\delta a_k^+ + v_k^\delta a_{k+\pi}^+, \quad c_k = u_k^\delta a_k - v_k^\delta a_{k+\pi} \tag{2.8a}$$

for $\mathcal{H}_\delta$ and

$$c_k^+ = u_k^\gamma a_k^+ + v_k^\gamma a_{-k}, \quad c_k = u_k^\gamma a_k - v_k^\gamma a_{-k}^+ \tag{2.8b}$$

for $\mathcal{H}_\gamma$.

The free-fermion representations of the spin Hamiltonians (1.1) and (1.2) are characterized by the one-particle spectra ω_k^δ: and ω_k^γ, respectively, given in (2.5). In zero magnetic field, they are isomorphic. As shown in fig. 1, the one-particle spectrum at $h = 0$ is characterized by an excitation gap at the wave number $k_0 = \pi/2$. The Fermi level is at zero energy; the ground state of $\mathcal{H}_g$ has all fermion states at $|k| < k_0$ empty and those at $k_0 < |k| < \pi$ occupied.

If we define the size of the one-particle energy gap Δ_1^g to be the minimum energy required to create or destroy a single fermion starting from the ground state, then we have $\Delta_1^\delta = \delta$ and $\Delta_1^\gamma = \gamma$ at $h = 0$.

As a magnetic field is turned on, the one-particle spectra of the two models develop in quite different ways. In the alternating chain, the one-particle spectrum ω_k^δ simply moves to higher energies with its shape unchanged. The one-particle gap has the following field dependence:

$$\Delta_1^\delta = \begin{cases} \delta - h, & 0 \le h \le \delta, \\ 0, & \delta \le h \le 1, \\ h - 1, & h \ge 1, \end{cases} \tag{2.9}$$

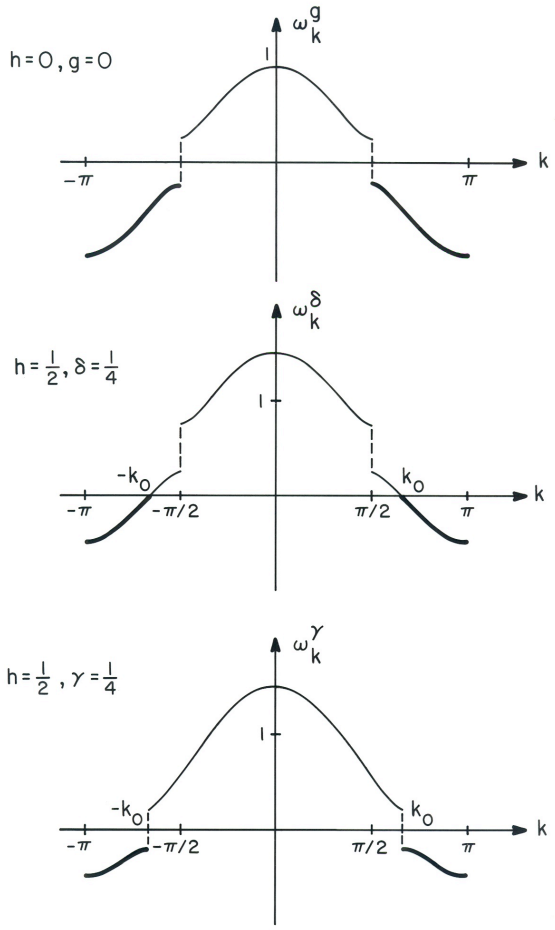

Figure 1. Single-particle spectra for the XY chain at $T = 0$ as functions of the wave number k. Shown are the zero-field, isotropic uniform case (top), and the alternating (middle) and anisotropic (bottom) cases for $h = \frac{1}{2}$ with alternation and anisotropy parameters $\delta = \frac{1}{4}$ and $\gamma = \frac{1}{4}$, respectively. Filled states are indicated by heavy lines, empty states by light lines. k_0 is the Fermi wave number.

as illustrated in fig. 2. The Fermi wave number k_0 moves from $\pi/2$ toπ as h increases through the gapless phase: $k_0 = \pi/2 + \arcsin\sqrt{(h^2 - \delta^2)/(1 - \delta^2)}$. Thus, there are two critical fields $h_G = \delta$, $h_c = 1$ in this model separating a gapless intermediate phase from two phases with an energy gap.

In the anisotropic chain the magnetic field has the effect of distorting the function ω_k^γ; the wave number k_0, separating the upper and the lower branch depends on the field as follows: $k_0 = \pi/2 + \arcsin(h)$ for $0 \le h \le 1$. At $h = h_c = 1$, which is the only critical field of this system, the lower branch of ω_k^γ disappears. The one-particle gap has the following field dependence:

$$\Delta_1^\gamma = \begin{cases} \gamma\big[1 - h^2/(1-\gamma^2)\big]^{1/2}, & 0 \le h \le 1-\gamma^2, \\ |h-1|, & h \ge 1-\gamma^2. \end{cases} \tag{2.10}$$

In this case it vanishes only at the critical field $h_c = 1$ as illustrated in fig. 2. Note that the minimum of $|\omega_k^\gamma|$, which determines Δ_1^γ occurs at a wave number

$$k_\Delta = \begin{cases} \arccos\big(h/(\gamma^2-1)\big), & 0 \le h \le 1-\gamma^2, \\ \pi, & h \ge 1-\gamma^2. \end{cases} \tag{2.11}$$

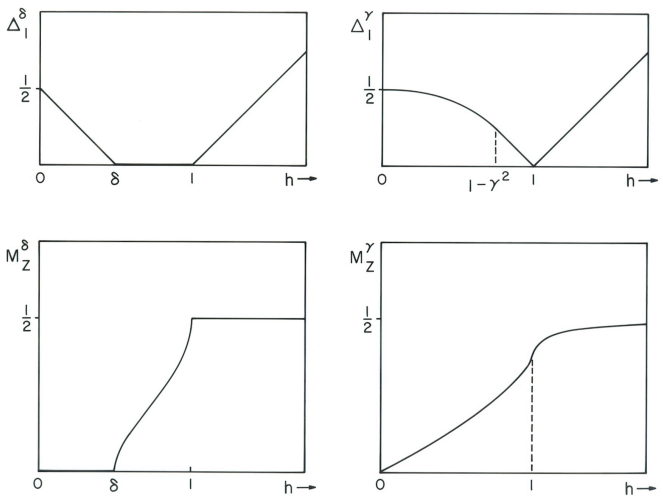

Figure 2. Single-particle energy gaps Δ_1^g (top) and magnetizations M_z^g, (bottom) for the alternating (left) and anisotropic (right) XY chains at $T = 0$ as functions of applied field h, with alternation and anisotropy parameters $\delta = \frac{1}{2}$ and $\gamma = \frac{1}{2}$ respectively.

For $0 < h < 1$, k_Δ differs from the wave number k_0, where the one-particle spectrum (2.5b) is discontinuous (this effect is, however, too small to be seen in fig. 1).

At this point we should remark that the relevant energy gap depends on the physical quantity under consideration. For the dynamic structure factor $S_{zz}(q,\omega)$ defined in (4.1) below, which is the main object of the present study, the relevant gap is the gap of two-particle excitations. The reason for this is that $S_{zz}(q,\omega)$ can be expressed in terms of a fermion density-density correlation function $\langle a_k^+(t)a_{k+q}(t)a_{k'}^+a_{k'-q}\rangle$ as explained in section 4 [14,51-53].

There are three processes contributing to the two-particle spectrum: two-particle excitations, two-hole excitations, and particle-hole excitations. In the case of $\mathcal{H}_\gamma$, all three processes contribute to $S_{zz}(q,\omega)$; the relevant gap is therefore twice the one-particle gap: $\Delta_{zz}^\gamma = 2\Delta_1^\gamma$. In the alternating case ($\mathcal{H}_\delta$), on the other hand, only particle-hole excitations contribute to $S_{zz}(q,\omega)$. The relevant gap Δ_{zz}^δ is therefore not simply related to Δ_1^δ of (2.11). For $0 \le h \le h_c$, we have $\Delta_{zz}^\delta = 2\delta\Theta(\delta - h)$ whereas for $h > h_c$ particle-hole excitations no longer exist at $T = 0$ because the fermion band ω_k^δ is empty.

By contrast, the dynamic structure factors $S_{xx}(q,\omega)$ and $S_{yy}(q,\omega)$ are much more complicated objects in the fermion representation, involving m-particle excitations with m arbitrarily large [53-57]. The relevant excitation gap may be different for these quantities in some cases.

3. Static properties

Before we proceed to our main theme, which is the study of dynamic correlation functions for the two models (1.1) and (1.2) it is helpful and informative to understand the behavior of various static quantities, in particular their $T = 0$ critical properties. From this we obtain the information necessary to understand the qualitative changes occurring in the dynamic properties at the critical fields h_G and h_c in the alternating chain and at the critical field h_c in the anisotropic chain.

3.1. Energy, magnetization and susceptibility

The thermodynamic properties of the two models (1.1) and (1.2) have been studied previously [12,13,15,16,21,22]. Here we briefly review the results for the ground state energy per spin

$$E^g(h) = \langle \mathcal{H}_g \rangle / N, \tag{3.1}$$

the $T = 0$ magnetization per spin in the field direction

$$M_z^g(h) = -\partial E^g/\partial h, \tag{3.2}$$

and the corresponding susceptibility per spin

$$\chi_{zz}^g(h) = -\partial^2 E^g/\partial h^2. \tag{3.3}$$

Some of these quantities are presented in closed form for the first time here.

The ground state energy of the anisotropic chain is obtained from (3.1) with (2.4) as

$$\begin{aligned} E^\gamma(h) &= -\frac{1}{2\pi}\int_0^\pi dk \sqrt{(h+\cos k)^2+\gamma^2\sin^2 k} \\ &= \frac{1}{\pi(1-\gamma^2)}\left[\gamma(\gamma^2-1)E\left(\frac{\beta}{\gamma}\right)+h^2\gamma\, K\left(\frac{\beta}{\gamma}\right)-\frac{h^2}{\gamma}\,\Pi\left(\frac{\gamma^2-1}{\gamma^2},\frac{\beta}{\gamma}\right)\right], \end{aligned} \tag{3.4}$$

from which the magnetization and the susceptibility functions are calculated by use of (3.2) and (3.3), respectively. The results are the following:

$$M_z^\gamma(h) = \frac{h}{\pi\gamma(1-\gamma^2)}\left\{\Pi\left(\frac{\gamma^2-1}{\gamma^2},\frac{\beta}{\gamma}\right)-\gamma^2 K\left(\frac{\beta}{\gamma}\right)\right\}, \tag{3.5}$$

$$\chi_{zz}^\gamma(h) = \frac{\gamma}{\pi\beta^2}\left\{K\left(\frac{\beta}{\gamma}\right)-E\left(\frac{\beta}{\gamma}\right)\right\}, \tag{3.6}$$

where K, E, Π are complete elliptic integrals of the first, second and third kind, and $\beta = \sqrt{h^2-1+\gamma^2}$ [58]. For the evaluation of these results a relation between elliptic integrals of the first and third kind was derived (see appendix).

Note that the special value $h = h_{\rm N} = \sqrt{1-\gamma^2}$ of the field forms a natural boundary at which β changes from an imaginary number to a real number. For $h \le h_{\rm N}$, then, we can use an imaginary modulus transformation to rewrite eqs. (3.4)-(3.6) obtaining

$$E^\gamma(h) = \frac{1}{\pi\sqrt{1-h^2}}\big\{(1-h^2)\big[K(k_1)-E(k_1)\big]-\Pi(h^2/(h^2-1),k_1)\big\}, \tag{3.7}$$

$$M_z^\gamma(h) = \frac{1}{\pi h\sqrt{1-h^2}}\big\{(h^2-1)\big[K(k_1)+\Pi(h^2/(h^2-1),k_1)\big\}, \tag{3.8}$$

$$\chi_{zz}^\gamma(h) = \frac{\sqrt{1-h^2}}{\pi(1-\gamma^2-h^2)}\left\{E(k_1)-\frac{\gamma^2}{1-h^2}K(k_1)\right\}, \tag{3.9}$$

with $k_1 = \sqrt{(1-\gamma^2-h^2)/(1-h^2)}$. Some prominent special cases of these results are summarized in table 1.

A typical magnetization curve ($\gamma = \frac{1}{2}$) is depicted in fig. 2. It starts out linearly in h and exhibits a singularity with infinite slope at $h = h_c = 1$, then gradually saturates as h is further increased. The corresponding susceptibility has a logarithmic divergence at h_c. The critical magnetization $M_z^\gamma(h_c)$ as given in the bottom row of table 1 approaches the saturated value $M_z^\gamma = \frac{1}{2}$ as the anisotropy goes to zero ($\gamma \to 0$). In this limit, the susceptibility has a square root divergence as $h \to h_c^-$.

Note that these thermodynamic quantities have no singularity at $h = h_{\rm N}$ although the system displays very peculiar properties here: the ground state reduces to a product state of single-site spin wave functions [59,60].

For the case of the alternating chain, the ground state energy $E^\delta(h)$, the magnetization $M_z^\delta(h)$, and the susceptibility $\chi_{zz}^\delta(h)$ are calculated from (3.1)-(3.3) with (2.4) as [21,22,25]

$$\begin{aligned} E^\delta(h) &= \frac{1}{\pi}\int_{k_0}^\pi dk\Big[h-\sqrt{\cos^2 k+\delta^2\sin^2 k}\Big]-\frac{1}{2}h \\ &= -\frac{1}{\pi}\,E\left(\pi(1/2-M_z^\delta),\sqrt{1-\delta^2}\right)-hM_z^\delta, \end{aligned} \tag{3.10}$$

$$M_z^\delta(h) = \begin{cases} 0, & 0 \le h \le \delta, \\ \frac{1}{\pi}\arcsin\sqrt{\frac{h^2-\delta^2}{1-\delta^2}}, & \delta \le h \le 1, \\ \frac{1}{2}, & 1 \le h, \end{cases} \tag{3.11}$$

$$\chi_{zz}^\delta(h) = \frac{h}{\pi}\left[(1-h^2)(h^2-\delta^2)\right]^{-1/2}\Theta(h-\delta)\Theta(1-h), \tag{3.12}$$

where $k_0 = \pi/2 + \pi M_z^\delta$ is the Fermi wave number as defined in section 2.

Table 1. The ground state energy (E^γ), magnetization (M_z^γ) and susceptibility (χ_{zz}^γ), for special cases of the anisotropic chain with an applied field (h) in the z-direction. γ is the anisotropy parameter described in the text.

γ	h	E^γ	M_z^γ	χ_{zz}^γ
0	$0 \le h \le 1$	$-\frac{h}{\pi}\arcsin h - \frac{1}{\pi}\sqrt{1-h^2}$	$\frac{1}{\pi}\arcsin h$	$\frac{1}{\pi\sqrt{1-h^2}}$
0	$h \ge 1$	$-\frac{1}{2}$	$\frac{1}{2}$	0
1	$0 \le h \le 1$	$\frac{1}{\pi}\left[(1-h^2)K(h) - 2E(h)\right]$	$\frac{1}{\pi h}\left[E(h) - (1-h^2)K(h)\right]$	$\frac{1}{\pi h^2}\left[K(h) - E(h)\right]$
1	$h \ge 1$	$\frac{h}{\pi}\left[\left(1-\frac{1}{h^2}\right)K\left(\frac{1}{h}\right) - 2E\left(\frac{1}{h}\right)\right]$	$\frac{1}{\pi}E\left(\frac{1}{h}\right)$	$\frac{1}{\pi h}\left[K\left(\frac{1}{h}\right) - E\left(\frac{1}{h}\right)\right]$
$0 \le \gamma \le 1$	0	$-\frac{1}{\pi}E\left(\sqrt{1-\gamma^2}\right)$	0	$\frac{E\left(\sqrt{1-\gamma^2}\right) - \gamma^2 K\left(\sqrt{1-\gamma^2}\right)}{\pi(1-\gamma^2)}$
$0 \le \gamma \le 1$	h_N	$-\frac{1}{2}$	$\frac{1}{2}\sqrt{\frac{1-\gamma}{1+\gamma}}$	$\frac{1}{4\gamma}$
$0 \le \gamma \le 1$	h_c	$-\frac{1}{\pi}\left[\gamma + (1-\gamma^2)^{-1/2}\right.$	$\frac{1}{\pi\sqrt{1-\gamma^2}}$	∞
		$\left.\times \arcsin\sqrt{1-\gamma^2}\right]$	$\times \arcsin\sqrt{1-\gamma^2}$	

A typical magnetization curve($\delta = \frac{1}{2}$) is shown in fig. 2. It stays zero up to h_G, then increases gradually and reaches saturation at h_c. The corresponding susceptibility has square-root divergences as h approaches h_G or h_c from within the gapless phase. It is interesting to note here that in the 1D $S = \frac{1}{2}$ XY model, where the exchange interaction is both anisotropic and alternating, the susceptibility has, in general, logarithmic divergences at two critical fields which correspond to h_G and h_c in the special case considered here [22].

In the limit $\delta = 0$ the lower critical field h, goes to zero and the corresponding singularity in the thermodynamic quantities disappears. For this case, the results of the isotropic uniform chain given in the first row of table 1 are recovered.

In the dimer limit $\delta = 1$ we have $M_z^\delta = \frac{1}{2}\Theta(h-1)$ and $\chi_{zz}^\delta = \frac{1}{2}\delta(h-1)$, reflecting the spin flip at $h_g = h_c = 1$.

3.2. Ordering in competition

The presence of exchange anisotropy and exchange alternation in the models (1.1) and (1.2) respectively, cause different types of spin orderings in the ground state of the system, which will be described in the following. In both cases the presence of an external magnetic field perpendicular to the xy-plane tends to counteract these orderings by gradually aligning the spins in the z-direction. Both types of orderings are finally destroyed as h reaches the critical strength h_c.

In the anisotropic chain, the ground state exhibits spontaneous magnetic long-range order in the xy-plane at $h < h_c$ in the form of a sublattice magnetization [16]

$$\bar{M}_x = \lim_{R\to\infty} |\langle S_l^x S_{l+R}^x\rangle|^{1/2} = \frac{1}{\sqrt{2(1+\gamma)}}\left[\gamma^2(1-h^2)\right]^{1/8}, \quad h \le h_c. \tag{3.13}$$

This is also reflected in the fact that the ground state is two-fold degenerate at $h < h_c$. With increasing h, the sublattice magnetization is progressively suppressed and finally disappears at h_c. Here the excitation continuum touches down to zero (see fig. 2) causing critical-point fluctuations, and the ground state changes from a doublet to a singlet. In the isotropic limit $\gamma = 0$, there is no spontaneous long-range order. The spectrum is gapless for $0 \le h \le h_c$ corresponding to a line of critical points. In the alternating case, the ordering situation is more complex. The ground state of $\mathcal{H}_\delta$ exhibits no spontaneous ($h = 0$) long-range order, magnetic or nonmagnetic. Spontaneous long-range order in the alternating chain arises only in the framework of a more general model, such as the model in which the positions of the magnetic ions belonging to the chain are no longer fixed but are assumed to be part of a 3D harmonic lattice, and where the exchange interaction varies with the average separation between them.

As far as $T = 0$ properties are concerned such a system can be modeled by a Hamiltonian of the form [61]

$$\bar{\mathcal{H}}_\delta = \sum_{l=1}^{N}\left[J(w_{l,l+1})\left\{S_l^x S_{l+1}^x + S_l^y S_{l+1}^y\right\} + hS_l^z + cw_{l,l+1}^2\right] \tag{3.14}$$

in generalization of (1.2). Here $w_{l,l+1} = R_{l+1} - R_l - a$, where R_l, denotes the position of the I-th magnetic ion in the undistorted lattice with lattice spacing a. To be specific, let us make the plausible assumption of a linear dependence on the distorted amplitude of the exchange coupling:

$$J(w_{l,l+1}) = 1 - \alpha w_{l,l+1}. \tag{3.15}$$

In this model the uniform ground state with $w_{l,l+1} = 0$ may become unstable against spontaneous dimerization characterized by

$$\alpha w_{l,l+1} = (-1)^l \delta. \tag{3.16}$$

In order to verify this, we determine the minimum energy of the Hamiltonian (3.14) for variable δ:

$$U^\delta(h) = E^\delta(h) + c\alpha^{-2}\delta^2. \tag{3.17}$$

The first term in (3.17), which is the ground state energy (3.10) of $\mathcal{H}_\delta$, is plotted in fig. 3 as a function of δ for various h. We observe that for all $h < h_c$, this quantity decreases upon dimerization. For $\delta \ll 1$ we have

$$E^\delta(h) - E^\delta(h)|_{\delta=0} \simeq \begin{cases} -\frac{1}{2\pi}\delta^2\left[\ln\left(\frac{4}{\delta}\right) - \frac{1}{2}\right], & 0 < h \le \delta, \\ -\frac{1}{2\pi}\delta^2\left[\ln\left(\frac{1+\sqrt{1-h^2}}{h}\right) - \sqrt{1-h^2}\right], & \delta < h < 1, \\ 0, & h \ge 1. \end{cases} \tag{3.18}$$

From (3.17) and (3.18) it is evident that the dimerized state is energetically favored over the uniform state not only at $h = 0$ but also at small nonzero h. Specifically for $c\alpha^{-2} \gg 1$, we have to distinguish three regimes: for $0 \le h \le h_0 \simeq 2\exp(-2\pi c\alpha^{-2})$ the energy function $U^\delta(h)$ has a global minimum at $\delta = \pm 2h_0$, which favors the dimerized state over the uniform state. In this regime the ground state of (3.14) breaks the translational symmetry of the interaction Hamiltonian $\bar{\mathcal{H}}_\delta$.

In the regime $h \ge 2h_0$, $U^\delta(h)$ has a single minimum at $\delta = 0$ corresponding to the uniform state. In the intermediate regime $h_0 \le h \le 2h_0$, U^δ has a local minimum at $\delta = 0$ and a global minimum at $\delta \simeq \pm 2h_0$. In this regime, one might therefore expect the appearance of hysteresis effects upon variation of the magnetic field in various quantities which are sensitive to the dimerization. Thus

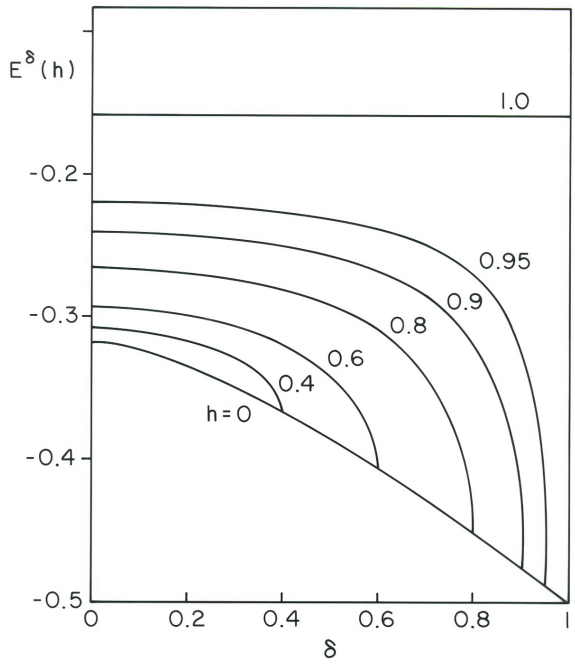

Figure 3. Ground state energy of the alternating XY chain as a function of the alternation parameter δ for various values of applied field h.

again, the spontaneous long-range order is increasingly suppressed and, finally, destroyed by an applied magnetic field. Whereas the long-range order in the anisotropic case was associated with the spontaneously broken reflection symmetry in spin space, the long-range order in $\bar{\mathcal{H}}_\delta$ is associated with the spontaneously broken translational symmetry along the chain. This type of long-range order makes its appearance in the magnetic properties; e.g. in the form of an alternating nearest-neighbor correlation function. This may serve for the construction of a magnetic order parameter of the form

$$C_\mu^\delta(h) \equiv |\langle S_l^\mu S_{l+1}^\mu - S_l^\mu S_{l-1}^\mu \rangle|, \quad \mu = x, y, z. \tag{3.19}$$

Since the translational ordering of a spin-Peierls system is intrinsically 3D in character, caused by the coupling of a 1D spin chain to a 3D lattice, it generally persists at $T > 0$. At nonzero T, however, the simple Hamiltonian (3.14) has to be replaced by an interacting 3D spin-phonon Hamiltonian which is no longer amenable to an exact analysis.

We should remark at this point that physical realizations of quasi-1D alternating spin systems are not necessarily the effect of a spontaneous lattice distortion but may be a consequence of the intrinsic crystallographic structure of the compound. In such systems, the alternation parameter δ is not field dependent.

$$\begin{aligned} C_x^\delta(h) = C_y^\delta(h) &= \left| \frac{\partial}{\partial \delta} E^\delta(h) \right| = \frac{\delta}{\pi} \int_{k_0}^{\pi} dk \frac{\sin^2 k}{\sqrt{\cos^2 k + \delta^2 \sin^2 k}} \\ &= \frac{\delta}{\pi(1-\delta^2)} \left[F\left(\frac{\pi}{2} - \pi M_z^\delta, \sqrt{1-\delta^2}\right) - E\left(\frac{\pi}{2} - \pi M_z^\delta, \sqrt{1-\delta^2}\right) \right], \end{aligned} \tag{3.20}$$

$$C_z^\delta(h) = \frac{2\delta}{\pi^2}\int_0^{\pi-k_0} dk' \int_{k_0}^{\pi} dk \frac{\sin^2 k\, \cos^2 k' + \cos^2 k\, \sin^2 k'}{\sqrt{[\cos^2 k + \delta^2 \sin^2 k][\cos^2 k' + \delta^2 \sin^2 k']}}$$
$$= \frac{4\delta}{\pi^2(1-\delta^2)^2}\left[F\left(\frac{\pi}{2} - \pi M_z^\delta, \sqrt{1-\delta^2}\right) - E\left(\frac{\pi}{2} - \pi M_z^\delta, \sqrt{1-\delta^2}\right)\right]$$
$$\times \left[-\delta^2 F\left(\frac{\pi}{2} - \pi M_z^\delta, \sqrt{1-\delta^2}\right) + E\left(\frac{\pi}{2} - \pi M_z^\delta, \sqrt{1-\delta^2}\right)\right]. \tag{3.21}$$

These quantities, of course, vanish in the uniform limit $\delta = 0$ for arbitrary h. For fixed $\delta \neq 0$, on the other hand, they are nonzero and constant for $0 \leq h \leq \delta$. Here, the system is locked into the singlet phase with an energy gap. The ground state wave function is not affected by the presence of the field. Upon further increase of the field, the system enters the gapless phase. Here $C_\mu^\delta(h)$ decreases continuously, reaching zero at the critical field. In the context of a spin-Peierls system, of course, δ itself is a function of the field which goes to zero at a value $h \simeq h_0$, much smaller than h_c, and is paralleled by the vanishing of the magnetic order parameters $C_\mu^\delta(h)$.

4. Dynamic properties

In this section we investigate the zero-temperature dynamical properties of the anisotropic and alternating XY chains. As in the preceding discussion of their static properties, our aim is to point out both their similarities and their differences. A quantity which contains detailed and experimentally most useful information is the dynamic structure factor

$$S_{\mu\mu}(q,\omega) = N^{-1}\sum_{ll'} \mathrm{e}^{-\mathrm{i}q(l-l')} \int_{-\infty}^{+\infty} dt\, \mathrm{e}^{\mathrm{i}\omega t}\big[\langle S_l^\mu(t) S_{l'}^\mu\rangle - \langle S_l^\mu(t)\rangle\langle S_{l'}^\mu\rangle\big], \tag{4.1}$$

where $\mu = x, y, z$. We shall therefore concentrate our discussion of dynamics on the properties of this function.

As already mentioned in section 2, the time-dependent correlation function $\langle S_l^z(t) S_{l'}^z\rangle$ of the two models (1.1) and (1.2) can be expressed as a density-density correlation function of noninteracting fermions. With use of the relations of section 2, it is straightforward to derive general integral expressions for $\langle S_l^z(t) S_{l'}^z\rangle$ or for its wave-number-dependent counterpart [62]

$$\langle S_q^z(t) S_{-q}^z\rangle \equiv N^{-1}\sum_{kk'} \langle \mathrm{e}^{\mathrm{i}\mathcal{H}t} a_k^+ a_{k+q} \mathrm{e}^{-\mathrm{i}\mathcal{H}t} a_{k'}^+ a_{k'-q}\rangle. \tag{4.2}$$

By Fourier transform, the following integral expressions for the dynamic structure factors $S_{zz}(q,\omega)$ at $T = 0$ of the two models (1.1) and (1.2) are then inferred. For the anisotropic chain we have

$$S_{zz}^\gamma(q,\omega) = \frac{1}{2}\int_0^\pi dk\big[1 - f^\gamma(k,q)\big]\delta\big(\omega - \epsilon^\gamma(k,q)\big), \tag{4.3a}$$

with

$$\epsilon^\gamma(k,q) = |\omega_{k-q/2}^\gamma| + |\omega_{k+q/2}^\gamma|, \tag{4.3b}$$

$$f^\gamma(k,q) = \frac{\big[h + \cos(k-q/2)\big]\big[h + \cos(k+q/2)\big] - \gamma^2 \sin(k-q/2)\sin(k+q/2)}{|\omega_{k-q/2}^\gamma||\omega_{k+q/2}^\gamma|} \tag{4.3c}$$

with ω_k^γ from (2.5b).

The general expression for the alternating chain is somewhat more complex:

$$S_{zz}^\delta(q,\omega) = \frac{1}{2}\int_{k_1}^{k_2} dk\big[1 - f^\delta(k,q)\big]\delta\big(\omega - \epsilon_+^\delta(k,q)\big) + \frac{1}{2}\int_{k_3}^{k_4} dk\big[1 - f^\delta(k,q)\big]\delta\big(\omega - \epsilon_-^\delta(k,q)\big), \tag{4.4a}$$

where

$$\epsilon_\pm^\delta(k,q) = ||\omega_{k-q/2}^\delta - h| \pm |\omega_{k+q/2}^\delta - h||, \tag{4.4b}$$

$$f^\delta(k,q) = \frac{\cos(k+q/2)\cos(k-q/2) + \delta^2 \sin(k+q/2)\sin(k-q/2)}{|\omega^\delta_{k-q/2} - h||\omega^\delta_{k+q/2} - h|}, \tag{4.4c}$$

and (assuming $0 \le q \le \pi$)

$$k_1 = \frac{\pi}{2} + \pi M_z^\delta + \frac{q}{2}, \quad k_2 = \frac{3\pi}{2} - \pi M_z^\delta + \frac{q}{2}, \tag{4.4d}$$

$$k_3 = \begin{cases} \dfrac{3\pi}{2} - \pi M_z^\delta - \dfrac{q}{2}, & q \le \pi - 2\pi M_z^\delta, \\ \dfrac{\pi}{2} + \pi M_z^\delta + \dfrac{q}{2}, & q \ge \pi - 2\pi M_z^\delta, \end{cases} \tag{4.4e}$$

$$k_4 = \begin{cases} \dfrac{3\pi}{2} - \pi M_z^\delta + \dfrac{q}{2}, & q \le 2\pi M_z^\delta, \\ \dfrac{3\pi}{2} + \pi M_z^\delta - \dfrac{q}{2}, & q \ge 2\pi M_z^\delta, \end{cases} \tag{4.4f}$$

with $M_z^\delta(h)$ from (3.11). Note that the second term in (4.4a) is nonzero only for $\delta < h < 1$; i.e. in the gapless phase. Furthermore, in zero field the two expressions (4.3) and (4.4) are almost isomorphic. The only difference is a sign in the numerator of $f(k,q)$.

Before we proceed to a detailed analysis of the structure of these functions, we should like to remark that the dynamic structure factors $S_{xx}(q,\omega)$ and $S_{yy}(q,\omega)$ of the XY chain cannot be expressed in terms of free-fermion density-density correlation functions [63], for it was shown that these quantities involve excitations of arbitrarily many fermions, not just two-particle excitations as in the case of $S_{zz}(q,\omega)$. Nevertheless, the results of ref. [53-57] indicate that the two-particle excitations give a significant, if not a dominant, contribution to the $T = 0$ dynamic structure factors $S_{xx}(q,\omega)$ and $S_{yy}(q,\omega)$ or related functions.

4.1. Two-particle spectrum and $S_{zz}(q,\omega)$ at $h = 0$

It is useful to start the analysis of the functions $S^g_{zz}(q,\omega)$, $g = \gamma, \delta$ with the analysis of the two-particle spectra $\epsilon^g(k,q)$; they comprise all excitations which contribute to $S^g_{zz}(q,\omega)$.

At $h = 0$, the two-particle spectra (4.3b) and (4.4b) of the two models are isomorphic. This spectrum is shown in fig. 4 for a typical value of the parameter $g = \gamma, \delta$. It consists of two partly overlapping continua $\mathcal{C}_+$ and $\mathcal{C}_-$, which are bounded by the branches

$$\epsilon_0(q) = (1+g)\sin q, \tag{4.5a}$$

$$\epsilon_1(q) = 2\sqrt{\sin^2\frac{q}{2} + g^2\cos^2\frac{q}{2}}, \tag{4.5b}$$

$$\epsilon_2(q) = 2\sqrt{\cos^2\frac{q}{2} + g^2\sin^2\frac{q}{2}}, \tag{4.5c}$$

as indicated in the figure. The boundary $\epsilon_0(q)$ exists only for $q_c \le q \le \pi - q_c$, where

$$q_c = 2\arctan\sqrt{g}. \tag{4.6}$$

The two-particle excitation gap is $\Delta_2^g(h=0) = 2g$ in agreement with the results of section 2. In order to evaluate $S^g_{zz}(q,\omega)$ explicitly we have to rewrite the δ-function in (4.3a) or (4.4a) explicitly as a function of k, whereupon the integral is trivially performed. The solution for the anisotropic case was presented and discussed previously in ref. [64]. The calculation for the alternating case is very similar. The explicit expressions for the $T = 0$ dynamic structure factors $S^\gamma_{zz}(q,\omega)$ and $S^\delta_{zz}(q,\omega)$ are the following:

$$S^g_{zz}(q,\omega) = S^g_+(q,\omega) + S^g_-(q,\omega) \tag{4.7a}$$

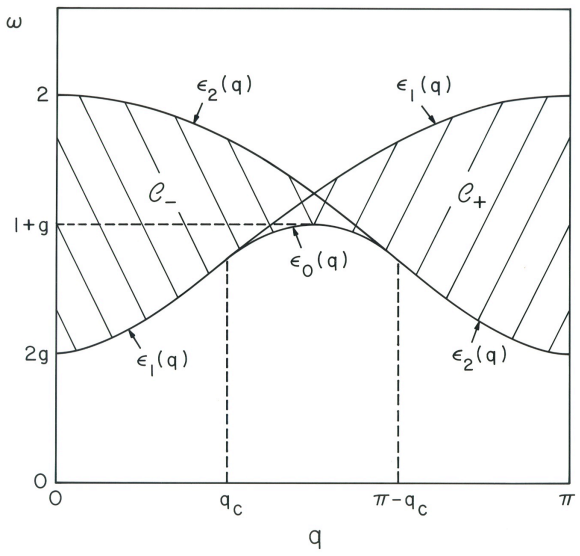

Figure 4. Two-particle excitation continua $\mathcal{C}_+$ and $\mathcal{C}_-$ for the zero-field XY chain at $T = 0$ with alternation or anisotropy parameter $g = \frac{1}{2}$. The continua overlap in the double cross-hatched region. The boundary ϵ_0 joins the boundary ϵ_1 (ϵ_2) smoothly at wave number $q = q_c$ ($q = \pi - q_c$).

where $S^g_\pm(q,\omega)$ is nonzero for $(q,\omega) \in \mathcal{C}_\pm$ and

$$S^g_\pm(q,\omega) = z^g_\pm(q,\omega)/e^g_\pm(q,\omega), \tag{4.7b}$$

$$e^g_\pm(q,\omega) = T^g(q,\omega)\frac{\sqrt{2(1+g^2)\sin^2 q - \omega^2(1+\cos^2 q) \mp 2\cos q\, T^g(q,\omega)}}{2\sin^2 q}, \tag{4.7c}$$

$$T^g(q,\omega) = \left[\omega^2 - (1-g)^2\sin^2 q\right]^{1/2}\left[\omega^2 - (1+g)^2\sin^2 q\right]^{1/2}, \tag{4.7d}$$

for $g = \gamma, \delta$ and

$$z^\delta_\pm(q,\omega) = \left(4\sin^2\frac{q}{2}\right)^{-1}\left\{\omega^2 - (1+\delta^2)\sin^2 q \pm T^\delta(q,\omega)\right\}, \tag{4.7e}$$

$$\begin{aligned} z^\gamma_\pm(q,\omega) = {} & \left[4(1-\gamma^2)\sin^2\frac{q}{2}\right]^{-1}\left\{\omega^2 - (1-\gamma^2)\sin^2 q \pm T^\gamma(q,\omega)\right\} \\ & - \gamma^2\left[4(1-\gamma^2)\cos^2\frac{q}{2}\right]^{-1}\left\{\omega^2 + (1-\gamma^2)\sin^2 q \mp T^\gamma(q,\omega)\right\}. \end{aligned} \tag{4.7f}$$

The two terms $S^\delta_+(q,\omega)$ and $S^\delta_-(q,\omega)$ in the dynamic structure $S^\delta_{zz}(q,\omega)$ for the alternating chain with $\delta = 0.1$ are depicted in figs. 5a and 5b, respectively. Corresponding illustrations for $S^\gamma_{zz}(q,\omega)$ of the anisotropic chain are found in fig. 5 of ref. [64], and therefore not reproduced here.

We observe that $S^\delta_{zz}(q,\omega)$ exhibits square-root divergences at all boundaries of the two-particle spectrum. They are caused by a divergent density of states

$$D^g(q,\omega) = \frac{1}{2}\int_0^\pi dk\,\delta\big(\omega - \epsilon^g(k,q)\big), \quad g = \gamma, \delta, \tag{4.8}$$

which, in explicit form, reads

$$D^g(q,\omega) = D^g_+(q,\omega) + D^g_-(q,\omega), \tag{4.9a}$$

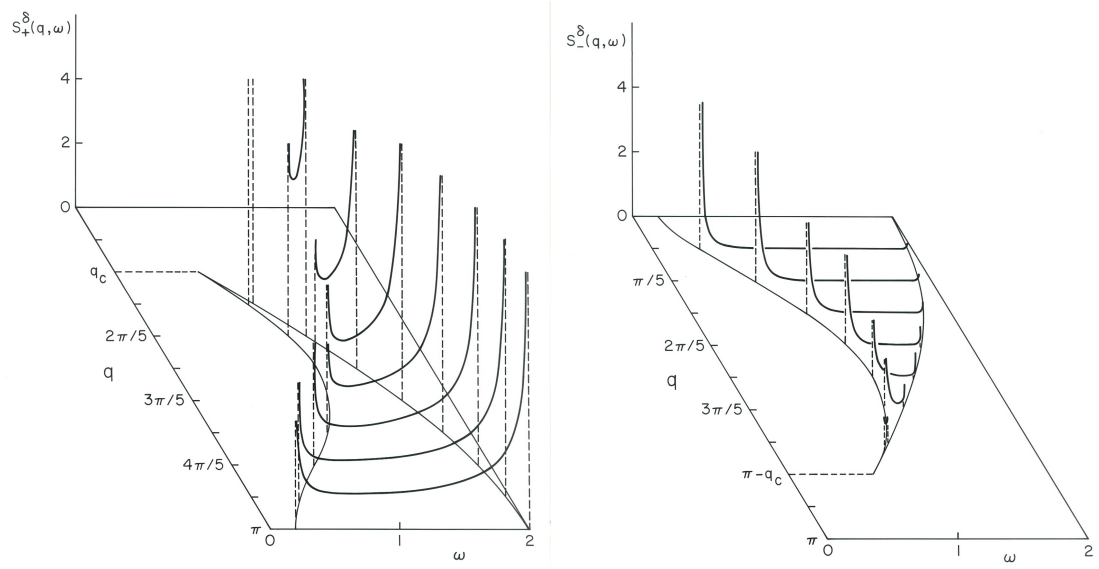

Figure 5. The dynamic correlation function $S^{\delta}_{zz}(q,\omega)$ of the $T = 0$ alternating XY chain for alternation parameter $\delta = 0.1$ in zero applied field at $q = n\pi/10$, $n = 0, 1, \ldots, 10$. The contributions from the two continua $\mathcal{C}_{\pm}$, are shown separately: $S^{\delta}_{+}(q,\omega)$ from $\mathcal{C}_{+}$ (a) and $S^{\delta}_{-}(q,\omega)$ from $\mathcal{C}_{-}$ (b).

with

$$D^{g}_{\pm}(q,\omega) = n^{g}_{\pm}(q,\omega)/e^{g}_{\pm}(q,\omega), \tag{4.9b}$$

$$n^{g}_{\pm}(q,\omega) = \frac{\omega^2 - (1+g^2)\sin^2 q \pm \cos q\, T^{g}(q,\omega)}{2\sin^2 q} \tag{4.9c}$$

with $T^{g}(q,\omega)$, $e^{g}_{\pm}(q,\omega)$ as defined above, all for $(q,\omega) \in \mathcal{C}_{\pm}$.

For the case shown in fig. 5, the divergence in $S^{\delta}_{zz}(q,\omega)$ at the boundary $\epsilon_2(q)$ is rather weak for $0 < q \leq \pi/2$. This is due to the smallness of the matrix elements in that area of (q,ω) space. The matrix elements relevant for $S^{g}_{zz}(q,\omega)$ in (q,ω) space are represented by the functions

$$M^{g}_{\pm}(q,\omega) = \frac{S^{g}_{\pm}(q,\omega)}{D^{g}_{\pm}(q,\omega)} = \frac{z^{g}_{\pm}(q,\omega)}{n^{g}_{\pm}(q,\omega)}. \tag{4.10}$$

Owing to the rotational symmetry of the Hamiltonian $\mathcal{H}_{\delta}$ about the z-axis, we have $S^{\delta}_{zz}(0,\omega) \equiv 0$. This is not the case for $S^{\gamma}_{zz}(0,\omega)$. Another major difference between the two results is that in the anisotropic case, the density-of-state divergence at $epsilon_2(q)$ is cancelled for $\pi - q_c \leq q \leq \pi$ by the vanishing of the matrix elements, causing $S^{\gamma}_{zz}(q,\omega)$ to go to zero there [64].

Naturally for $h = 0$ we have

$$\lim_{\gamma\to 0} S^{\gamma}_{zz}(q,\omega) = \lim_{\delta\to 0} S^{\delta}_{zz}(q,\omega) = 2\frac{\Theta\big(\omega - \sin q\big)\Theta\big(2\sin(q/2) - \omega\big)}{\sqrt{4\sin^2(q/2) - \omega^2}}. \tag{4.11}$$

4.2. $S^{\gamma}_{zz}(q,\omega)$ at $h \neq 0$

We now turn to the magnetic-field effects on the $T = 0$ dynamic structure factors $S^{g}_{zz}(q,\omega)$ of the two models. First we direct our attention to the anisotropic chain, and we begin by analyzing the special case $\gamma = 1$, which characterizes the transverse Ising model.

Following the same general approach as before, we find that the excitation spectrum is, in general, again composed of two partially overlapping continua, bounded by three branches

$$\epsilon_0(q) = 2\sin\frac{q}{2}\max(1,h), \tag{4.12a}$$

$$\epsilon_1(q) = 2\left|1 - 2h\cos\frac{q}{2} + h^2\right|^{1/2}, \tag{4.12b}$$

$$\epsilon_2(q) = 2\left|1 + 2h\cos\frac{q}{2} + h^2\right|^{1/2}, \tag{4.12c}$$

as illustrated in fig. 6 for a typical case. For $h \to 0$, the spectrum collapses into a single horizontal line at energy $\omega = 2$. This is a highly degenerate limiting case ($g = 1$) of the spectrum shown in fig. 4. With h increasing from zero, the branch $\epsilon_2(q)$, which becomes the upper boundary of continuum $\mathcal{C}_+$, moves (not rigidly) to higher energies. Simultaneously, the branch $\epsilon_1(q)$ moves (also with distortion) to lower energies for $q < q_c$, where

$$\cos\frac{q_c}{2} = \min\bigl(h, h^{-1}\bigr), \tag{4.13}$$

and to higher energies at $q > q_c$. At $q < q_c$ it forms the lower bound of continuum $\mathcal{C}_+$ and at $q > q_c$ the upper boundary of continuum $\mathcal{C}_-$. At q_c, $\epsilon_0(q)$, which is independent of h, branches off $\epsilon_1(q)$, forming the lower boundary of both continua for $q \le q \le \pi$. It is not present for $q < q_c$.

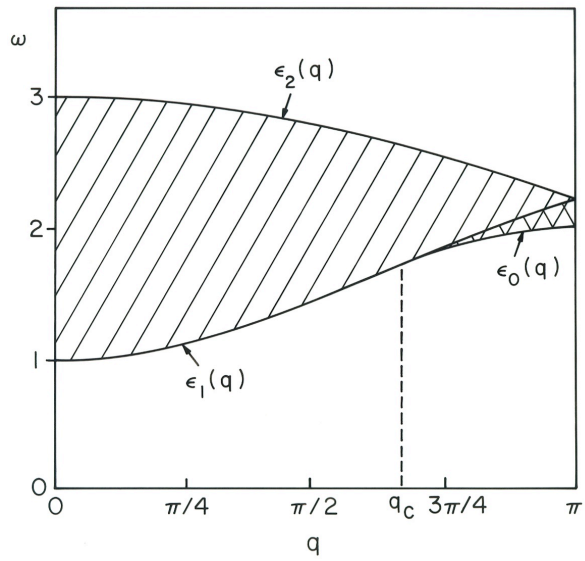

Figure 6. Two-particle excitation continua $\mathcal{C}_\pm$ for the $T = 0$ transverse king model with applied field $h = \frac{1}{2}$. $\mathcal{C}_-$ covers the entire continuum, whereas $\mathcal{C}_+$ exists only in the double cross-hatched region. The boundaries ϵ_0 and ϵ_1 join smoothly at q_c.

As h approaches the critical field $h_c = 1$, both $\epsilon_0(q)$ and $\epsilon_1(q)$ touch down to zero energy at $q = 0$: the excitation gap vanishes in agreement with the results of section 2. As h continues to increase beyond h_c, the gap reappears and the spectrum moves to higher energies, including the boundary $\epsilon_0(q)$ which was independent of h below h_c.

The explicit result for the dynamic structure factor $S^{TI}_{zz}(q,\omega)$ at $T = 0$ and arbitrary h can be expressed as follows:

$$S^{TI}_{zz}(q,\omega) = D^{TI}_+(q,\omega)M^{TI}_+(q,\omega) + D^{TI}_-(q,\omega)M^{TI}_-(q,\omega), \tag{4.14a}$$

where the two terms are nonzero only in the two continua $\mathcal{C}_+$ and $\mathcal{C}_-$, respectively, and

$$D_{\pm}^{TI}(q,\omega) = \frac{1}{2h}\left|\frac{\sin(k_\pm - q/2)}{\sqrt{h^2+2h\cos(k_\pm - q/2)+1}} + \frac{\sin(k_\pm + q/2)}{\sqrt{h^2+2h\cos(k_\pm + q/2)+1}}\right|^{-1}, \tag{4.14b}$$

$$M_{\pm}^{TI}(q,\omega) = 1 - f^{\gamma=1}(k_\pm, q), \tag{4.14c}$$

with $f^\gamma(k,q)$ from (4.3c) and where $k_\pm$ is determined by

$$\cos k_\pm = \frac{-\omega^2\cos(q/2)}{4h\sin^2(q/2)} \mp \left(\frac{\omega^2}{4h^2\sin^2(q/2)} - 1\right)^{1/2}\left(\frac{\omega^2}{4\sin^2(q/2)} - 1\right)^{1/2}. \tag{4.14d}$$

The behavior of $S_{zz}^{TI}(q,\omega)$ as a function of ω for fixed $q = \pi/5$ and $4\pi/5$ at $h = \frac{3}{4}$, 1, and $\frac{4}{3}$ is illustrated in fig. 7. The shapes of these curves are understood to result from the following properties of the function (4.14).

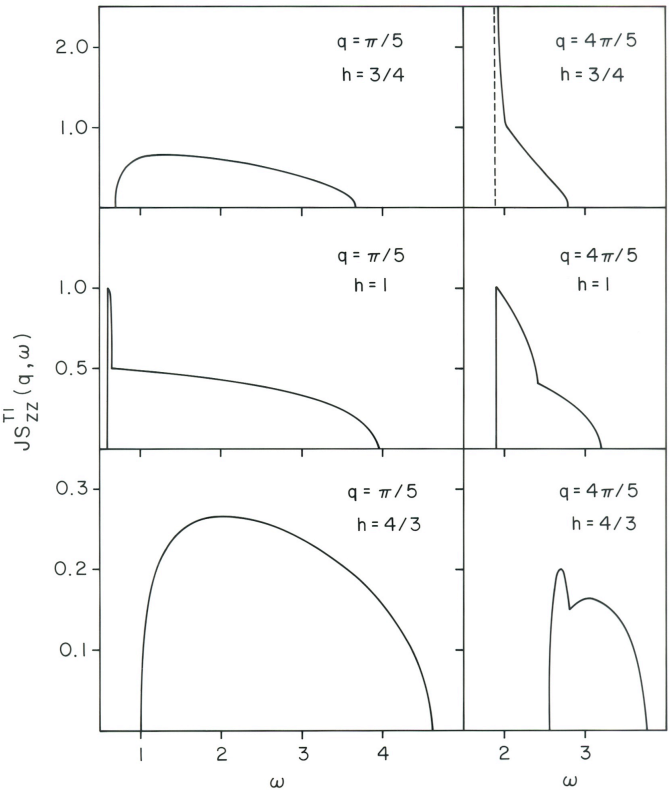

Figure 7. The dynamic correlation function $JS_{zz}^{TI}(q,\omega)$ of the $T = 0$ transverse Ising model for $q = \pi/5$ (left) and $4\pi/5$(right) with $J = 1$. Shown are the cases for applied field $h = \frac{3}{4}$ (top), 1 (middle), and $\frac{4}{3}$ (bottom).

At $0 < h < 1$, $S_-^{TI}(q,\omega)$ goes to zero at $\epsilon_2(q)$ for all q and at $\epsilon_1(q)$ for $0 \le q \le q_c$. For $q_c < q \le \pi$, $S_+^{TI}(q,\omega)$ goes to zero at $\epsilon_1(q)$) whereas $S_-^{TI}(q,\omega)$ is finite on $\epsilon_1(q)$; both have square-root divergences along $\epsilon_0(q)$. Hence, for $0 < q < q_c$, $S_{zz}^{TI}(q,\omega)$ is basically a featureless bulge with a peak toward $\epsilon_1(q)$ and going to zero at both boundaries $\epsilon_1(q)$ and $\epsilon_2(q)$. For $q_c < q \le \pi$, on the other hand, $S_{zz}^{TI}(q,\omega)$ varies continuously from the zero at $\epsilon_2(q)$ to the divergence at $\epsilon_0(q)$; there is, though, a discontinuity in the slope of $S_{zz}^{TI}(q,\omega)$ along $\epsilon_1(q)$.

At the critical field $h_c = 1$, the divergence at $\epsilon_0(q)$, which is now the common lower boundary of both continua for all q (since $q_c = 0$), has disappeared. $S^{TI}_{zz}(q,\omega)$ is equal to one at this boundary. There is still a discontinuity in the slope at $\epsilon_1(q)$, however.

For $h = h_c$, the result (4.14) can be rewritten in greatly simplified form as [57]

$$S^{TI}_{zz}(q,\omega) = \frac{\sqrt{16\cos^2(q/4) - \omega^2}}{8\cos^2(q/4)}\Theta\big(4\cos(q/4) - \omega\big)\Theta\big(\omega - 2\sin(q/2)\big) + \frac{\sqrt{16\sin^2(q/4) - \omega^2}}{8\sin^2(q/4)}\Theta\big(4\sin(q/4) - \omega\big)\Theta\big(\omega - 2\sin(q/2)\big). \tag{4.15}$$

At $h > 1$, both terms $S^{TI}_{+}(q,\omega)$ and $S^{TI}_{-}(q,\omega)$ of the dynamic structure factor (4.14) go to zero at either boundary of the continua $\mathcal{C}_+$ and $\mathcal{C}_-$, respectively. As before, for $0 < q < q_c$, $S^{TI}_{zz}(q,\omega)$ is a featureless bulge; for $q_c < q \leq \pi$, it is continuous, but has a slope discontinuity at $\epsilon_1(q)$. As q increases, the height of the peak diminishes, and $S^{TI}_{zz}(q,\omega)$ becomes more symmetrical. As h increases, $S^{TI}_{zz}(q,\omega)$ slowly decreases in both width and height.

Many of the characteristic features of $S^{TI}_{zz}(q,\omega)$ outlined above are, in fact, typical for the dynamic structure factor $S^{\gamma}_{zz}(q,\omega)$ for the generic case of the anisotropic chain in a magnetic held, which, however, is much harder to analyze.

Some peculiar properties, which are less typical for the generic case, are exhibited by two other special cases of $\mathcal{H}_\gamma$ for which $S^{\gamma}_{zz}(q,\omega)$ was analyzed previously.

In the isotropic limit $\gamma = 0$, the spectrum is gapless throughout the regime $0 \leq h \leq 1$ as already noted in section 2. A peculiarity of this model is that one of the two wave numbers for which the excitation spectrum touches down to zero energy is $q_c = 2\arccos(h)$. As h increases from 0 to 1, this "soft mode" moves continuously from the Brillouin zone boundary to the zone center, thus indicating the presence of some incommensurate structure in the ground state wave function [65].

The special case with $h = h_{\mathrm{N}} \equiv \sqrt{1-\gamma^2}$, $0 \leq \gamma \leq 1$, corresponds to a situation where the ground state can be expressed as a direct product of single-site spin wave functions, reflecting a spin-flop state with no correlated fluctuations. In spite of this unusually simple ground state, the dynamic structure factors $S_{\mu\mu}(q,\omega)$, $\mu = x, y, z$, exhibit, in general, nontrivial properties except for $\gamma = 1$, $0 \leq q \leq \pi$ and for $q = \pi$, $0 \leq \gamma \leq 1$, where the exact result for $S_{\mu\mu}(q,\omega)$ agrees with the spin-wave prediction [66].

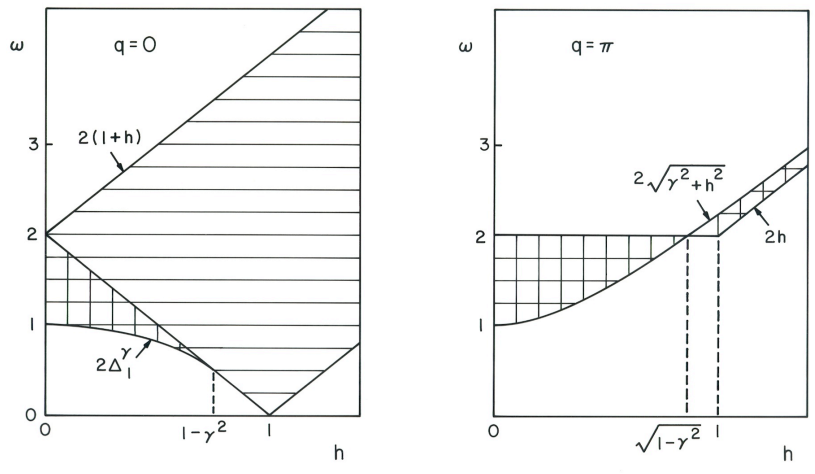

Figure 8. The two-particle continuum ω of the $T = 0$ anisotropic XY chain with anisotropy parameter $\gamma = \frac{1}{2}$ as a function of applied field h for $q = 0$ (left) and π (right). $2\Delta^{\gamma}_1$ is the two-particle energy gap.

The analysis of $S_{zz}(q,\omega)$ for the most general case of the anisotropic XY chain reaches a degree of mathematical complexity which would make a discussion very lengthy without the benefit of adding qualitatively new features.

We therefore restrict our discussion to one simple aspect which should help us to establish the connections between the various special cases considered above. This is the h-dependence of the two-particle spectrum at $q = 0$ and $q = \pi$, as illustrated in fig. 8 for $\gamma = \frac{1}{2}$.

For $q = 0$, we observe that at $h = 0$ the continuum, which can be identified with the continuum $\mathcal{C}_-$ fig. 4, splits into two sheets, one of which disappears at $h = 1 - \gamma^2$. The remaining continuum becomes gapless at $h = h_c$. The energy of the lowest branch is the two-particle gap $\Delta_2^\gamma = 2\Delta_1^\gamma$ in agreement with (2.10).

For $q = \pi$, the continuum at $h = 0$ is identified with the continuum $\mathcal{C}_-$ of fig. 4. The width of this continuum shrinks to a point at $h = h_{\mathrm{N}} = \sqrt{1-\gamma^2}$ in agreement with the result of ref. [60] quoted above and then increases again up to the critical field h„ before it shrinks again and disappears asymptotically for large h.

4.3. $S^\delta_{zz}(q,\omega)$ at $h \neq 0$

The situation described already in subsection 4.1 for the zero-field case of the alternating chain remains unchanged for $0 < h < \delta$. This is understood by noting that the magnetization M_z^δ, which is the only parameter of expression (4.4) for $S^\delta_{zz}(q,\omega)$ depending on the field, is zero over this range of h. Likewise, $S^\delta_{zz}(q,\omega) \equiv 0$ in this regime, in accordance with the known result that the ground state is ferromagnetic with all spins aligned parallel to the field. The interesting situation at $h \neq 0$ thus pertains to the regime $\delta \leq h \leq 1$, corresponding to the gapless phase of the alternating chain, where some basic structural changes occur.

The most prominent feature clearly is the appearance of a new excitation continuum at low energies for $\delta \leq h \leq 1$, within the lower band of ω_k^δ. It is profitable, however, to begin the discussion with the magnetic-field effects occurring in $S^\delta_{zz}(q,\omega)$ at the energies corresponding to the upper continua $\mathcal{C}_+$ and $\mathcal{C}_-$ of fig. 4.

The magnetic field enters the general expression (4.4) for the dynamic structure factor $S^\delta_{zz}(q,\omega)$ only via the integration boundaries in (4.4a). This has the simplifying consequence that $S^\delta_{zz}(q,\omega)$ for arbitrary h can be expressed in the form

$$S^\delta_{zz}(q,\omega) = \frac{1}{2}\Big[p_+(q,\omega)S^\delta_+(q,\omega) + p_-(q,\omega)S^\delta_-(q,\omega) + \bar{p}_+(q,\omega)\bar{S}^\delta_+(q,\omega) + \bar{p}_-(q,\omega)\bar{S}^\delta_-(q,\omega)\Big], \quad (4.16)$$

where the functions $S^\delta_\pm(q,\omega)$, which determine the $h = 0$ dynamic structure factor, are given in (4.7) and the functions $\bar{S}^\delta_\pm(q,\omega)$, which will be determined incthe following and are also h-independent, represent the new low-energy excitation continua. The h-dependence in (4.16) is entirely contained in the four functions $p_\pm, \bar{p}_\pm$; $p_\pm$ can assume only the values 0, 1, 2, depending on the coverage with particle-hole excitations of a given area in (q,ω) space, whereas $\bar{p}_\pm$ can assume only the values 0, 1, depending on the coverage of the appropriate low-energy continuum.

For the two upper continua $\mathcal{C}_+$ and $\mathcal{C}_-$, this coverage can be described in terms of the familiar h-independent continuum boundaries $\epsilon_0(q)$, $\epsilon_1(q)$, $\epsilon_2(q)$ as defined in (4.5) and two new boundaries which depend on h as follows:

$$\epsilon_1'(q) = h + h^{-1}\Big\{\big[h^2\cos q - \sqrt{(h^2\delta^2)(1-h^2)}\,\sin q\big]^2 + \delta^2\sin^2 q\Big\}^{1/2}, \quad (4.17a)$$

$$\epsilon_2'(q) = \epsilon_1'(\pi - q) \quad (4.17b)$$

At $h = \delta$, the zero-field picture described in section 4.1 and illustrated in figs. 4 and 5 still holds. The spectrum for this case is shown again in fig. 9a, for $h = \delta = 0.5$, now including the degenerate branches $\epsilon_1'(q) = \epsilon_2'(q)$. There is double coverage everywhere in $\mathcal{C}_+$ and $\mathcal{C}_-$ corresponding to $p_\pm = 2$ for all $(q,\omega) \in \mathcal{C}_\pm$.

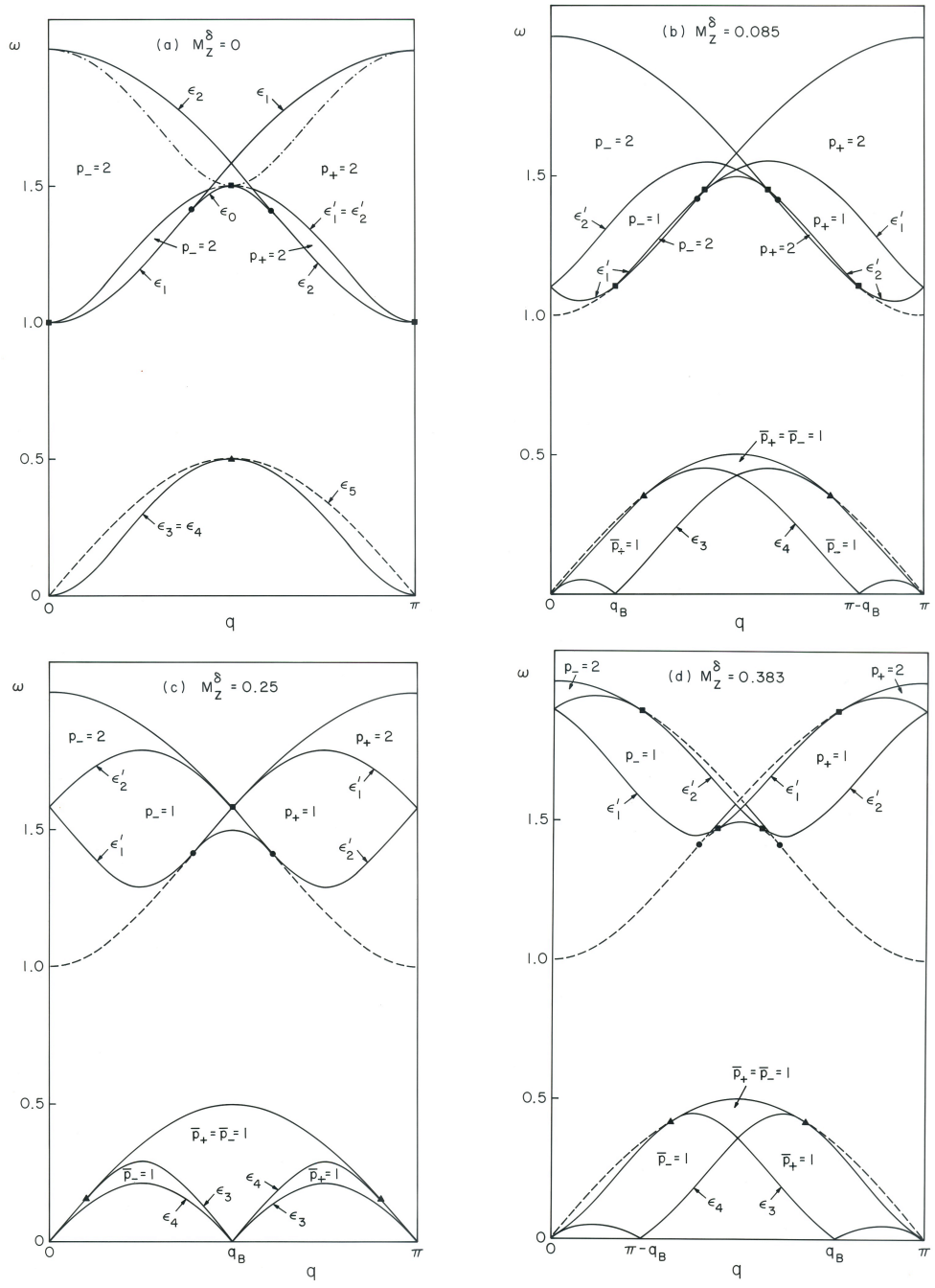

Figure 9. Two-particle excitation continua for the $T = 0$ alternating XY chain with alternation parameter $\delta = \frac{1}{2}$ in applied field h. External boundaries are given in the text, as are ϵ_1' and ϵ_2'. Values of $p_\pm$ and $\bar{p}_\pm$ indicate coverage of their respective continua by two-particle excitations. Coverage changes across ϵ_1' and ϵ_2', and is always zero outside the external boundaries. Solid circles are at q_c and $\pi - q_c$; solid triangles at q_A and $\pi - q_A$; solid squares show points where ϵ_1' or ϵ_2' touches an external boundary (which includes q_D and $\pi - q_D$ where applicable). Cases shown are: (a) $h \leq \delta$, $M_z^\delta = 0$ (dot-dashed line shows $\epsilon_1' = \epsilon_2'$ for $h \geq 1$, $M_z^\delta = \frac{1}{2}$); (b) $h = 0.55$, $M_z^\delta = 0.085$; (c) $h = 0.79$, $M_z^\delta = 0.25$; (d) $h = 0.95$, $M_z^\delta = 0.383$. Soft modes occur at wave numbers $q = 0, \pi, q_B, \pi - q_B$.

Upon increasing h slightly above the value $h = \delta$, the two branches $\epsilon_1'(q)$ and $\epsilon_2'(q)$ start to separate, giving rise to areas of single coverage ($p_\pm = 1$) and zero coverage ($p_\pm = 0$) in some areas of the continua $\mathcal{C}_\pm$. This situation is illustrated in fig. 9b for $h = 0.55$.

Note that $S^\delta_{zz}(q,\omega)$ now has discontinuities across either boundary $\epsilon_1'(q)$ or $\epsilon_2'(q)$. In areas of zero coverage, we have drawn the boundaries $\epsilon_0(q)$, $\epsilon_1(q)$, $\epsilon_2(q)$ as dashed lines in order to indicate the absence of the divergences in $S^\delta_{zz}(q,\omega)$ which are otherwise present all along these boundaries, as explained in subsection 4.1.

Fig. 9c shows the spectrum for $h = \sqrt{(1+\delta^2)/2}$ corresponding to a magnetization $M^\delta_z = \frac{1}{4}$ (half the saturation value). At this stage, there is no longer any spectral weight along the lower parts of the boundaries $\epsilon_1(q)$ and$\epsilon_2(q)$.

For $h > \sqrt{\delta}$, the areas of zero coverage start to include also the boundary $\epsilon_0(q)$ for$q < q_{\rm D}$ and $q > \pi - q_{\mathcal{D}}$, where

$$\tan q_{\rm D} = \frac{h^2+\delta}{\sqrt{(1-h^2)(h^2-\delta^2)}}, \quad \delta \le h \le 1. \tag{4.18}$$

Fig. 9d depicts the spectrum for h close to the critical field ($h = 0.95$). At this stage, stretches of the upper wings of the continuum boundaries $\epsilon_1(q)$ and $\epsilon_2(q)$ also lose their spectral weight. Double coverage is now restricted to the two uppermost corners of the continua $\mathcal{C}_\pm$.

Finally, as h reaches the critical field $h_c = 1$, the two branches $\epsilon_1'(q)$ and $\epsilon_2'(q)$ merge again, and the spectral weight disappears throughout the upper continua: $p_\pm(q,\omega) = 0$ for all $(q,\omega) \in \mathcal{C}_\pm$. The degenerate branches $\epsilon_1'(q) = \epsilon_2'(q)$ for $h = 1$ are shown dot-dashed in fig. 9a.

We now turn to the low-energy spectrum, which is absent at $h < \delta$. For $\delta < h < 1$, it consists of two partly overlapping continua bounded by the three branches

$$\epsilon_3(q) = \big|h - h^{-1}\big\{\big[h^2\cos q - \sqrt{(h^2-\delta^2)(1-h^2)}\sin q\big]^2 + \delta^2\sin^2 q\big\}^{1/2}\big|, \tag{4.19a}$$

$$\epsilon_4(q) = \epsilon_3(\pi - q), \tag{4.19b}$$

$$\epsilon_5(q) = (1-\delta)\sin q, \tag{4.19c}$$

as indicated in the sequence of figs. 9a-d. The h-independent branch $\epsilon_5(q)$ assumes the role of a common upper boundary of both continua in the restricted regime $q_{\rm A} < q < \pi - q_{\rm A}$, where

$$\tan q_{\rm A} = \frac{|h^2-\delta|}{\sqrt{(h^2-\delta^2)(1-h^2)}}, \quad \delta \le h \le 1. \tag{4.20}$$

At $h = \delta^+$, this low-energy spectrum makes its appearance in $S^\delta_{zz}(q,\omega)$ first in the form of the single degenerate branch $\epsilon_3(q) = \epsilon_4(q)$ as shown in fig. 9a.

Upon increasing h, this branch spreads into the two continua as shown in fig. 9b. This spectrum is characterized by four zero-frequency modes at wave numbers $q = 0$, $q_{\rm B}$, $\pi - q_{\rm B}$ and π, respectively, where

$$q_{\rm B} = 2\pi M^\delta_z. \tag{4.21}$$

Thus, two of these modes move continuously through the Brillouin zone in opposite directions as h increases through the gapless phase. As the critical field $h_c = 1$ is approached from below, the two continua contract again into a single branch of the same shape as at $h = \delta$, and disappear.

This part of the dynamic structure factor $S^\delta_{zz}(q,\omega)$ can also be expressed, according to (4.16) in terms of an h-independent function

$$\bar S^\delta(q,\omega) = \frac{1}{2}\int_0^\pi dk\big[1 + f^\delta(k,q)\big]\delta\big(\omega - \epsilon^\delta_-(k,q)\big) = \frac{1}{2}\big[\bar p_+ \bar S^\delta_+(q,\omega) + \bar p_- S^\delta_-(q,\omega)\big], \tag{4.22}$$

where

$$\bar S^\delta_\pm(q,\omega) = \frac{\bar z^\delta_\pm(q,\omega)}{\bar e^\delta_\pm(q,\omega)}, \tag{4.23a}$$

$$\bar z^\delta_\pm(q,\omega) = \Big(4\sin^2\frac{q}{2}\Big)^{-1}\big\{-\omega^2 + (1+\delta^2)\sin^2 q \mp T^\delta(q,\omega)\big\}, \tag{4.23b}$$

and $\bar{e}^{\delta}_{\pm}(q,\omega) = e^{\delta}_{\pm}(q,\omega)$. The $\bar{p}_{\pm}$ are equal to one over their respective continua, and zero elsewhere. This results in finite discontinuities along $\epsilon_3(q)$ and $\epsilon_4(q)$. $\bar{S}^{\delta}_{\pm}(q,\omega)$ has a square-root divergence along $\epsilon_5(q)$ for $q_{\rm A} < q < \pi - q_{\rm A}$ and is finite everywhere else.

Acknowledgements

The authors have benefited from interesting discussions with J.C. Bonner, B.M. McCoy, J.H.H. Perk, and R.E. Shrock. This work was supported in part by U.S. National Science Foundation grants DMR-X0-10819 and PHY-81-91 IOA01. One of us (J.H.T.) acknowledges the support of a University of Rhode Island graduate student fellowship during part of this project. We have used a modified cmpj.sty style file.

A. A special relation among elliptic integrals of the third kind

In obtaining eq. (3.4) a relation has been used between an elliptic integral of the third kind with a modulus of a special form and elliptic integrals of the first and third kind with a simpler modulus. In the following, we present a derivation of this relation, which is quoted in eq. (A.7) below. Analogous relations for elliptic integrals of the first or second kind are already well known.

We begin with two standard relations among elliptic integral [58]:

$$(1-\alpha^2)(k^2-\alpha^2)\Pi(\alpha^2,k) + \alpha^2 k'^2 \Pi\left(\frac{k^2-\alpha^2}{1-\alpha^2},k\right) = k^2(1-\alpha^2)K(k), \tag{A.1}$$

and

$$\Pi(\phi,\alpha_1^2,k_1) = (1+k')\frac{(k^2-\alpha^2)\Pi(\theta,\alpha^2,k) + (\alpha_2^2-k^2)\Pi(\theta,\alpha_2^2,k)}{\alpha_2^2-\alpha^2}, \tag{A.2}$$

where $k'^2 = 1-k^2$, and

$$\begin{aligned} k_1 &= \frac{1-k'}{1+k'}, \quad \sin\phi = \frac{(1+k')\sin\theta\cos\theta}{\sqrt{1-k^2\sin^2\theta}}, \\ \alpha^2 &= \frac{(1+k')^2}{2}\left[k_1+\alpha_1^2 - \sqrt{(1-\alpha_1^2)(k_1^2-\alpha_1^2)}\right], \\ \alpha_2^2 &= \frac{(1+k')^2}{2}\left[k_1+\alpha_1^2 + \sqrt{(1-\alpha_1^2)(k_1^2-\alpha_1^2)}\right]. \end{aligned} \tag{A.3}$$

In relation (A.2) we take $\theta = \pi/2$, which gives complete elliptic integrals on the right-hand side. It is found by comparison with the results of independently obtained special cases for $M^{\delta}_z(h,\gamma)$ that $\phi = \pi$, rather than zero. Relation (A.2) becomes

$$2\Pi(\alpha_1^2,k_1) = (1+k')\Big[(k^2-\alpha^2)\Pi(\alpha^2,k) + (\alpha_2^2-k^2)\Pi(\alpha_2^2,k)\Big]/(\alpha_2^2-\alpha^2). \tag{A.4}$$

When k can be written in the form $k = 2\sqrt{l}/(l+1)$, it can be shown directly that

$$\alpha_2^2 = \frac{k^2-\alpha^2}{1-\alpha^2}, \quad \alpha_2^2 - k^2 = -\frac{\alpha^2 k'^2}{1-\alpha^2}. \tag{A.5}$$

The third of expressions (A.3) is easily solved for α_1^2, yielding

$$\alpha_1^2 = \frac{\alpha^2}{\alpha^2-1}\left[\frac{\alpha^2}{(1+k')^2} - k_1\right]. \tag{A.6}$$

Relations (A.1) and (A.4) can each be solved for $\Pi(\alpha_2^2,k)$ and the results equated, giving, after a little algebra,

$$\Pi\left(\alpha^2,\frac{2\sqrt{l}}{1+l}\right) = \frac{(1+k')\sqrt{(1-\alpha_1^2)(k_1^2-\alpha_1^2)}}{k^2-\alpha^2}\,\Pi(\alpha_1^2,k_1) + \frac{k^2(1+k_1)}{2(k^2-\alpha^2)}\,K(k_1), \tag{A.7}$$

where $k_1 = l$ for $l \leq 1$ and $1/l$ for $l > 1$. In obtaining eq. (A.7) use has also been made of the standard relation [58]

$$K\left(\frac{2\sqrt{l}}{1+l}\right) = (1+k_1)K(k_1).$$

References

1. C.N. Yang and C.P. Yang, Phys. Rev. **150** (1966) 321, **151** (1966) 258.
2. J. des Cloizeaux and J.J. Pearson, Phys. Rev. **128** (1962) 2131. J. des Cloizeaux and M. Gaudin, J. Math. Phys. **7** (1966) 1384.
3. G. Müller, H. Thomas, M.W. Puga and H. Beck, J. Phys. C**14** (1981) 3399. H. Beck and G. Müller, Sol. St. Comm. **43** (1982) 399.
4. T. Schneider, E. Stoll and U. Glaus, Phys. Rev. B **26** (1982) 1321.
5. F.D.M. Haldane, Phys. Rev. Lett. **45** (1980) 1358.
6. A. Luther and 1. Peschel, Phys. Rev. B **12** (1975) 3908. H.C. Fogedby, J. Phys. C **11** (1978) 4767.
7. G. Müller, H. Thomas, H. Beck and J.C. Bonner, Phys. Rev. B **24** (1981) 1429.
8. H.J. Mikeska, Phys. Rev. B **12** (1975) 2794.
9. N. lshimura and H. Shiba, Prog. Theor. Phys. **57** (1977) 1862, **63** (1980) 743.
10. J.D. Johnson and B.M. McCoy, Phys. Rev. A **6** (1972) 1613. J.D. Johnson and J.C. Bonner, Phys. Rev. B **22** (1980) 251. J.D. Johnson, Phys. Rev. A **9** (1974) 1743.
11. M. Takahashi and M. Suzuki, Prog. Theor. Phys. **48** (1972) 2187. M. Takahashi, Prog. Theor. Phys. **50** (1973) 1519, **51** (1974) 1348. M.W. Puga, J. Math. Phys. **21** (1980) 2307.
12. E. Lieb, T. Schultz and D. Mattis, Ann. Phys. (NY) **16** (1961) 407.
13. S. Katsura, Phys. Rev. **127** (1962) 1508. M.E. Fisher, J. Math. Phys. **4** (1963) 124. P. Pfeuty, Ann. Phys. (NY) **57** (1970) 79.
14. T. Niemeijer, Physica **36** (1967) 377.
15. B.M. McCoy, Phys. Rev. **173** (1968) 531.
16. E. Barouch and B.M. McCoy, Phys. Rev. A **3** (1971) 786.
17. F.D.M. Haldane, Phys. Rev. Lett. **50** (1983) 1153; Phys. Lett. **93A** (19X3) 464.
18. R. Botet and R. Jullien, Phys. Rev. B **27** (1983) 613.
19. J.C. Bonner and G. Müller, Phys. Rev. B **29** (1984) 5216.
20. S.T. Chui and K.B. Ma, Phys. Rev. B **27** (1983) 4515.
21. V.M. Kontorovich and V.M. Tsukernik, Sov. Phys. JETP **26** (1968) 687.
22. J.H.H. Perk, H.W. Capel, M.J. Zuilhof and T.J. Siskens, Physica **81A** (1975) 319.
23. J.C. Bonner and H.W.J. Blöte, Phys. Rev. B **25** (1982) 6959.
24. M.C. Cross and D.S. Fisher, Phys. Rev. B **19** (1979) 402.
25. L.N. Bulaevskii, Sov. Phys. JETP **17** (1963) 684.
26. J.C. Bonner, H.W.J. Blöte and J.D. Johnson, J. Appl. Phys. **50** (1979) 7379.
27. B.S. Shastry and B. Sutherland, Phys. Rev. Lett. **47** (1981) 964. F.D.M. Haldane, Phys. Rev. B **25** (1982) 4925.
28. M. Suzuki, Prog. Theor. Phys. **46** (1971) 1337.
29. R.J. Baxter, Ann. Phys. (NY) **70** (1972) 323; J. Stat. Phys. **9** (1973) 14.5.
30. J.L. van Hemmen and G. Vertogen, Physica **81A** (1975) 391.
31. G.O. Berim and A.R. Kessel, Physica **116A** (1982) 526, **117A** (1983) 603.
32. J.L. Black and V.J. Emery, Phys. Rev. B **23** (1981) 429.
33. M. Kohmoto, M. den Nijs and L.P. Kadanoff, Phys. Rev. B **24** (1981) 5229.
34. M.P.M. den Nijs, Phys. Rev. B **23** (1981) 6111.
35. J.P. Groen, T.O. Klaassen, N.J. Poulis, G. Müller. H. Thomas and H. Beck. Phys. Rev. B **22** (1980) 5369. J.P. Green. H.W. Capel, J.H.H. Perk, T.O. Klaassen and N.J. Poulis, Physica **97B** (1979) 126.
36. K.M. Diederix, H.W.J. Blöte, J.P. Groen, T.O. Klaassen and N.J. Poulis. Phys. Rev. B **19** (1979) 420.
37. J.W. Bray, L.V. Interrante, I.S. Jacobs, D. Bloch, D.E. Moncton, G. Shirane and J.C. Bonner, Phys. Rev. B **20** (1979) 2067.
38. J.C. Bonner, S.A. Friedberg, H. Kobayashi, D.L. Meier and H.W.J. Blöte, Phys. Rev. B **27** (1983) 248.
39. I.S. Jacobs, J.W. Bray, H.R. Hart Jr., L.V. Interrante, J.S. Kasper, G.D. Watkins, D.E. Prober and J.C. Bonner, Phys. Rev. B **14** (1976) 3036.

40. J.J. Smit, L.J. de Jongh, J.A.C. van Ooijen, J. Reedijk and J.C. Bonner, Physica **97B** (1979) 229.
41. D. Bloch, J. Voiron, J.C. Bonner, J.W. Bray, I.S. Jacobs and L.V. Interrante, Phys. Rev. Lett. **44** (1980) 294.
42. P.M. Duxbury, J. Oitmaa, M.N. Barber, A. van der Bilt, K.O. Joung and R.L. Carlin, Phys. Rev. B **24** (1981) 5149.
43. Y. Endoh, G. Shirane, R.J. Birgenau, P.M. Richards and S.L. Holt, Phys. Rev. Lett. **32** (1974) 170. I.U. Heilmann, G. Shirane, Y. Endoh, R.J. Birgenau and S.L. Holt, Phys. Rev. B **18** (1978) 3530.
44. H. Yoshizawa, K. Hirakawa, S.K. Satija and G. Shirane, Phys. Rev. B **23** (1981) 2298.
45. S.E. Nagler, W.J.L. Buyers, R.L. Armstrong and B. Briat, J. Appl. Phys. **52** (1981) 1971; Phys. Rev. B **27** (1983) 1784.
46. S.K. Satija, J.D. Axe, R. Gaura, R. Willett and C.P. Landee, Phys. Rev. B **25** (1982) 6855.
47. D.R. Taylor, Phys. Rev. Lett. **42** (1979) 1302.
48. M. D'Iorio, R.L. Armstrong and D.R. Taylor, Phys. Rev. B **27** (1983) 1664.
49. A short account of a previous comparative study of these two models, which is much more limited in scope, is found in ref. [26].
50. See e.g. refs. [23], [24] and [39] for extensive accounts of both theory and experiments on the spin-Peierls transition.
51. S. Katsura, T. Horiguchi and M. Suzuki, Physica **46** (1970) 67.
52. J.H.H. Perk, H.W. Capel and T.J. Siskens, Physica **89A** (1977) 304.
53. B.M. McCoy, E. Barouch and D.B. Abraham, Phys. Rev. A **4** (1971) 2331.
54. H.W. Capel and J.H.H. Perk, Physica **87A** (1977) 211. J.H.H. Perk and H.W. Capel, Physica **89A** (1977) 265, **100A** (1980) 1.
55. H.G. Vaidya and C.A. Tracy, Physica **92A** (1978) 1.
56. B.M. McCoy, J.H.H. Perk and R.E. Shrock, Nucl. Phys. **B220** [FSS] (1983) 35, 269.
57. G. Müller and R.E. Shrock, Phys. Rev. Lett. **51** (1983) 219; Phys. Rev. B **29** (1984) 288.
58. IS. Gradshteyn and I.M. Ryzhik. *Tables of Integrals, Series, and Products*, 4th ed. (Academic Press, New York, 1980). P.F. Byrd and M.D. Friedman, *Handbook of Elliptic Integrals for Engineers and Scientists*, 2nd ed. (Springer, New York, 1971).
59. J. Kurmann, H. Thomas and G. Müller, Physica **112A** (1982) 235.
60. J.H. Taylor and G. Müller, Phys. Rev. B **28** (1983) 1529.
61. The $h = 0$ case for this model was previously studied by P. Pincus, Solid State Commun. **9** (1971) 1971, with respect to the spin-Peierls transition.
62. Such expressions are found in ref. [14] for the anisotropic chain with arbitrary h and in ref. [52] for both the alternating and anisotropic chains at $h = 0$.
63. More precisely, $S_{xx}(q,\omega)$ and $S_{yy}(q,\omega)$ can be expressed in terms of fermion density-density correlation functions, but only for an interacting fermion system, which, in general, is not tractable on a rigorous basis.
64. M. Mohan and G. Müller, Phys. Rev. B **27** (1983) 1776.
65. A closed-form analytic expression for $S_{zz}(q,\omega)$ for $\gamma = 0$ and arbitrary h is found in eq. (2.3) of ref. [7] along with figures for the spectrum and the function itself.
66. A closed-form analytic expression for $S_{zz}(q,\omega)$ for this case is found in eq. (14) of ref. [60] along with figures for the spectrum and the function itself. Note, however, that the expression in square brackets in the numerator of eq. (14) should be raised to the $\frac{1}{2}$ power.